Residual Stresses

10.1 Introduction

10.1.1 Definition

The stresses existing in an elastic body in the absence of external forces or loads (thermal or mechanical) are termed as residual stresses. This can be appreciated further from the schematic illustrated in Fig. 10.1 which shows an irregular externally loaded two dimensional body. The external forces or loads are denoted by symbol F_i, where $i = 1–5$ and acts on a small region indicated by A. After removal of external forces or loads, two possible scenarios for the region denoted by letter A are: (a) there are no internal stresses, and (b) there are internal stresses present in the absence of external loads F_i. The stresses within the body in state (b) are termed as residual stresses.

10.1.2 Causes of Residual Stress

Residual stresses are a consequence of inhomogeneous thermal distribution and plastic deformation of different regions during processing of a component. This can arise due to complex thermal-metallurgical-mechanical interactions during processing of an elastic body. This aspect of residual stress is pictorially depicted in Fig. 10.2 (Inoue and Wang 1985). For the introduction of residual stresses in a given component it is not necessary for all the factors mentioned in Fig. 10.2 to be present simultaneously. For example, the heating and cooling of a plate may lead to generation of thermal stresses which can eventually lead to residual stresses. In general, uneven or inhomogeneous heating and cooling leads to the generation of residual stresses. However, microstructural changes due to transformations during isothermal heat treatment can also lead to residual stresses.

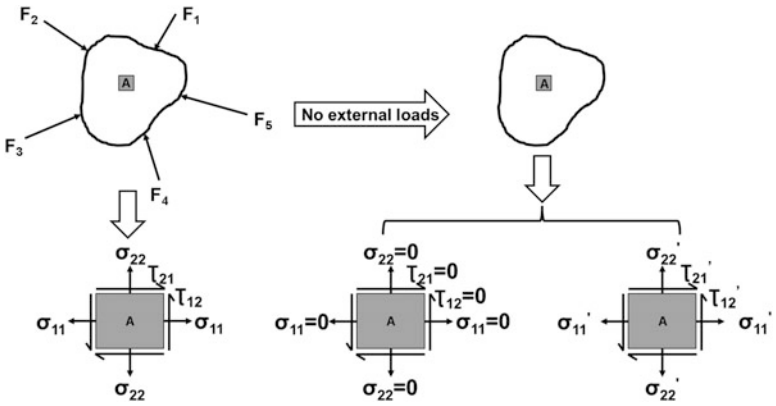

Fig. 10.1 A schematic illustration of definition of residual stresses

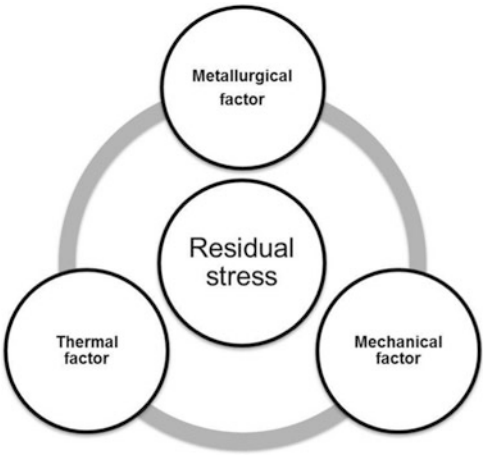

Fig. 10.2 Schematic illustration of residual stress development in an elastic body as a result of coupling between metallurgical, thermal, and mechanical factors

10.1.3 Types of Residual Stresses

Almost all manufacturing processes lead to generation of residual stresses which can differ in nature and scale. Figure 10.3 very broadly classifies residual stresses into two categories—macrostresses and microstresses. It further illustrates how industrial processes such as peening, cold hole expansion, bending and welding can lead to generation of macrostresses. Microstressess occur at much smaller scale than that of macrostresses. Processes which can lead to generation of microstresses are also illustrated in Fig. 10.3. All thermo-mechanical treatments which introduce macrostresses can also generate microstresses. In some cases it is quite possible that the two types of stresses coexist.

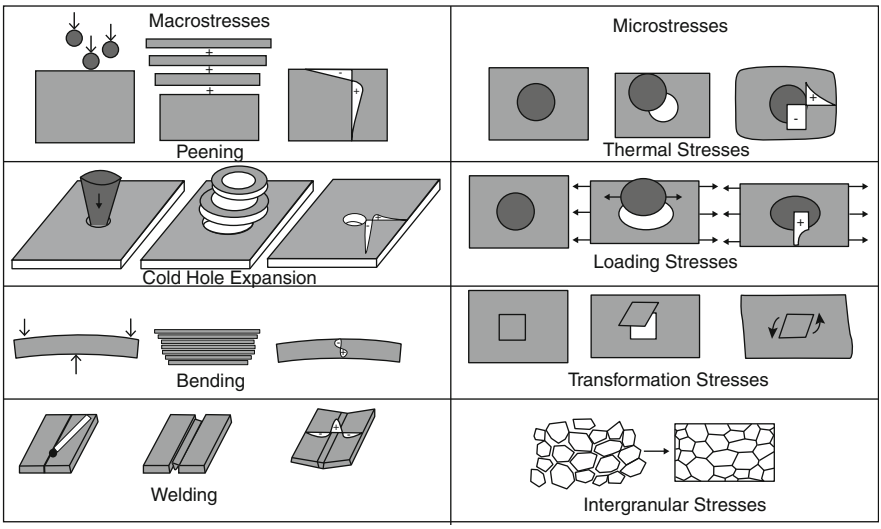

Fig. 10.3 A schematic of some industrial processes which lead to generation of residual stresses (adapted from Withers 2001)

Depending on the length scale residual stresses are again categorized based on the dimension over which they equilibrate: (a) Type I (equilibrium exists over the scale of the structure), (b) Type II residual stresses equilibrate over tens of grains, and (c) Type III exists at atomic scale (see Fig. 10.4). A rectangular box filled with grey color represents a component and shows the variation of Type I residual stress over the length of the entire structure. To represent Type II and Type III residual stresses, which are microscopic and submicroscopic in scale, a magnified image of a small white colored region in the grey colored rectangular box is shown next to it. Below this is shown variations of such stresses over the length of a few grains. These are type II residual stresses and an average value is also shown over the same dimension. Type III stresses are shown as variation of residual stresses within a grain and can exist due to the presence of defects like dislocations, precipitates, etc.

Type II and Type III are beyond the scope of the present book and only Type I residual stresses would be discussed which is relevant to welding processes in general and friction stir welding in particular.

10.1.4 Implications of Residual Stresses

Residual stresses can be beneficial or deleterious depending on the nature of stresses and the conditions considered. For example, the growth rate of a crack is accelerated when residual stresses are tensile and retards under compressive conditions (See Chap. 5 Figs. 5.12 and 5.15). This is a consequence of the effect on stress intensity at the crack tip given by

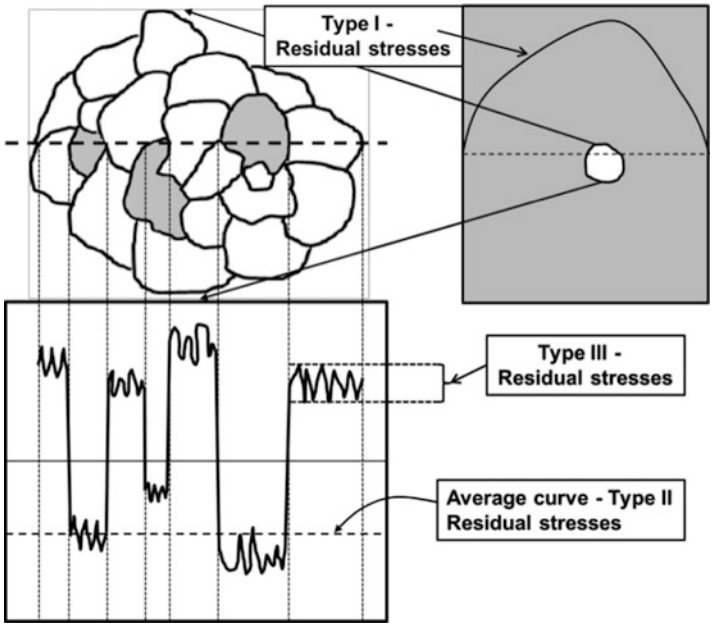

Fig. 10.4 A schematic illustration of different types of residual stresses commonly observed in functional materials (Adapted from Withers and Bhadeshia (2001))

Fig. 10.5 A through crack in an infinite plate illustrating the effect of residual stress on crack intensity factor; σ_{rs} = residual stress

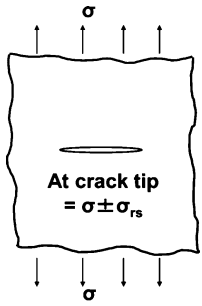

$$K_I = \sigma\sqrt{\pi a} \tag{10.1}$$

where K_I and σ are stress intensity factor and applied stress, respectively (Fig. 10.5). Depending on the magnitude and direction of residual stress σ reduces or increases by an equal amount. If K_I exceeds the K_{IC} (critical stress intensity factor—a material property), the crack propagates triggering a failure of the component. In such instances compressive residual stresses are beneficial, although the same is not true where buckling strength of the structure is of prime importance. Other properties which are influenced by the presence of residual stress include fatigue life, fracture toughness, stress corrosion cracking, etc. (Fig. 10.13).

10.2 Residual Stresses in Welding

During welding a concentrated heat source is applied along the weld centerline to form a joint. This heat source results in an intense thermal gradient in the material which causes inhomogeneous deformation of the workpiece being welded. Figure 10.6 schematically shows the temperature and thermal stress distribution at different positions (Fig. 10.6a) of the plate for a fusion welding process. Compared to other locations the peak temperature is highest at OO (Fig. 10.6c) which is just under the heat source and thermal stresses are close to zero. In case of friction stir welding, the region in close proximity to the tool has thermal stresses close to the yield stress of the alloy at that temperature. In the vicinity of the weld centerline along OO, the thermal stresses are compressive and on moving further towards the edge they turn tensile before tapering down to zero. Along the line BB (Fig. 10.6d) which is behind the moving heat source, the welded zone begins to cool down. The welded material tries to contract. However, the material surrounding the weld zone restricts it from doing so. Hence, this results in the generation of tensile stresses. The tensile thermal stress magnitude at location AA (Fig. 10.6e) is even higher since temperature at this location has reduced even further. Finally, at line CC (Fig. 10.6b) ahead of the heat source the plate is still at its initial temperature and thermal stresses are still zero.

At the end of welding cycle when the workpiece has cooled down sufficiently, the clamps restraining the workpiece are released and the thermal stresses

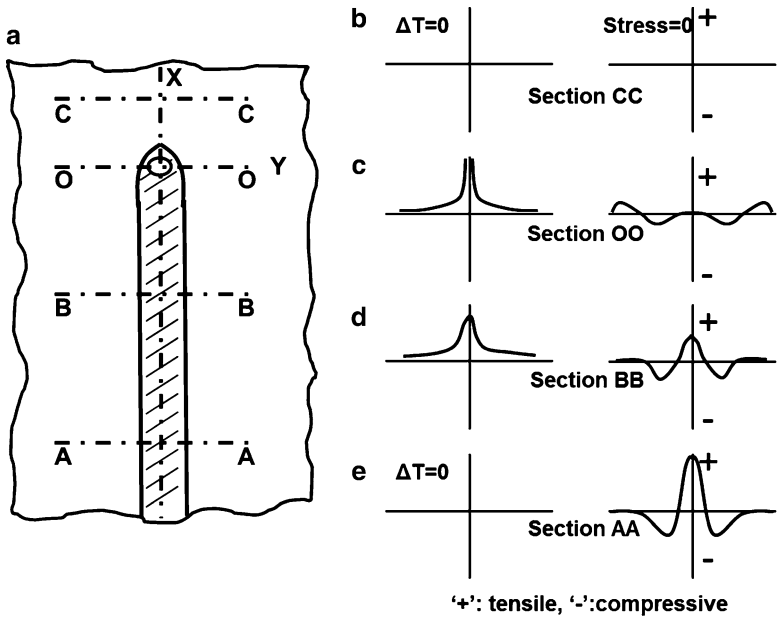

Fig. 10.6 Schematic showing temperature and thermal stress distribution at different regions of the plate being fusion welded (adapted from Masubuchi 1980a)

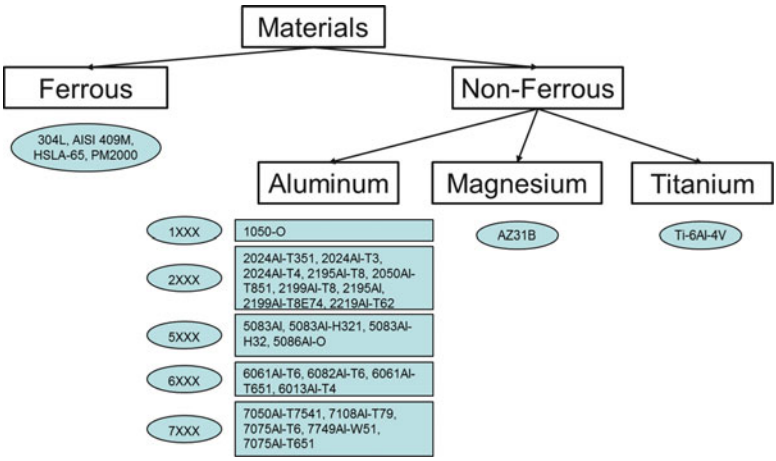

Fig. 10.7 An overview of the materials investigated for residual stress and distortion study in friction stir welding

redistribute themselves and result in residual stresses (and resulting in distortion). This generic description of thermal and residual stress development provides an insight in how such stresses develop during welding process. Later in this chapter, a schematic model is included to discuss the origin of residual stress during friction stir welding.

10.2.1 Residual Stresses in Friction Stir Welding

At the early stages of friction stir welding research, due to the solid state nature of the process the residual stress generated during joining was considered to be nominal. But, subsequent research indicates that a significant amount of residual stresses, sometime approaching the yield strength of the alloy can exist. The choice of friction stir welding process parameters controls the magnitude and distribution of residual stresses in friction stir welded structure. Section 10.5 discusses this aspect in greater detail. Among various parameters, one parameter is heat input which is defined as weld power per unit length. However, compared to other commercially available techniques, it is not possible to carry out friction stir welding at very high speed. So, even if the weld power requirement is low compared to other welding techniques, heat input becomes significant. Hence, consideration of total heat input per unit length suggests significant level of residual stresses.

Due to historical reason, the early research in residual stress and distortions is predominantly for aluminum alloys. Figure 10.7 provides an overview of the materials investigated for residual stress studies. Table 10.1 lists some of the aluminum alloys investigated so far. In addition, the processing parameters details and peak value of residual stresses observed along with the techniques used to

Table 10.1 A summary of processing parameters and residual stress measurement of friction stir welded aluminum alloys

Alloy	YS (MPa)	Tensile stress (max), MPa	Tensile RS (weld centerline), MPa	Tool traverse speed (mm/min)	Tool rotation rate (rpm)	Plate dimension (after joining)			Measurement technique	References
2024Al-T3	345	185	150	200	800	500	700	5	Neutron and synchrotron diffraction	Altenkirch et al. (2009a)
2195Al	215 (weld plate)	150	100	150	300	910	300	12.5	X-ray diffraction	Hatamleh (2009)
2024Al-T351	470	56	40	71.5	750	100	140	3	Cut-compliance technique	Fratini et al. (2009)
5083Al-H321	228	155	120	160	600	1,000	200	3.5	Slot sectioning stress relaxation method	Han et al. (2011
6061Al-T6	276	140	50	279		300	300	6	Neutron diffraction	Wang et al. (2000)
6013Al-T4	203	200	80	1,000	1,500			1.8	X-ray diffraction	Lemmen et al. (2010)
7075Al-T6	510	92	40	100	715				Cut-compliance technique	Buffa et al. (2008)
7449Al		200	200	250	225	1,000	300	12	Synchrotron diffraction	Altenkirch et al. (2008)
7075Al-T6	525 (BM), 390 (Nugget)	225	200	300	280			2	X-ray diffraction	Lemmen et al. (2010)
7108Al-T79	400	200	120	600					Ultrasonic wave technique	Gachi et al. (2009)

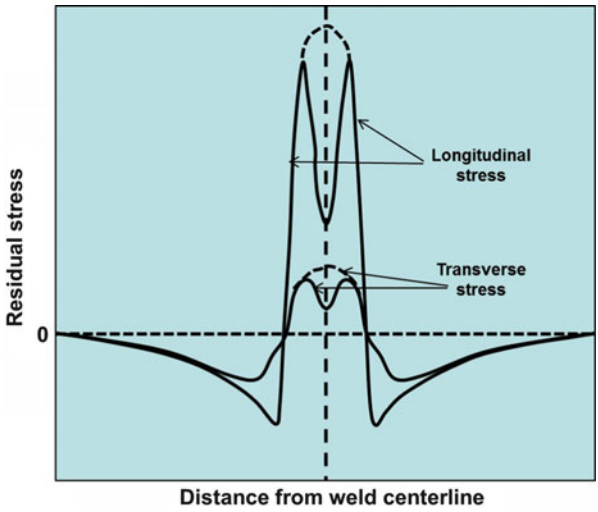

Fig. 10.8 Schematic showing the distribution and shape of residual stresses across the width of friction stir welded components

measure such stresses are included. Evidently, residual stresses in the welded structure are of considerable proportion with respect to the yield strength of the welded alloy. Such a level of residual stress in the friction stir welded structure is a matter of some concern from application point of view. Hence, every effort should be made to mitigate magnitude of residual stresses.

The general trend observed in terms of distribution and shapes of residual stress curves across the width of the weldments are shown in Fig. 10.8. Salient features of this distribution with respect to friction stir welded ferrous and non-ferrous alloys are:

- In general, longitudinal residual stresses are tensile in nature in welded region. Outside of the welded region it is compressive. It becomes asymptotically zero on moving towards the edge of workpiece.
- Overall, transverse residual stresses are also tensile in nature. The variation across the width of the weldments can be similar. However, in general, the magnitude of these stresses is smaller than the longitudinal residual stresses.
- Maximum longitudinal tensile stress mostly occur either in thermo-mechanically or heat-affected zones. In few instances, maximum longitudinal stresses have been found at weld centerline also.
- It leads to two different types of residual stress profile—M-shaped and inverted V- shaped profiles (Fig. 10.8).
- The residual stress curves can be approximated using following expression:

$$\sigma_x(y) = \sigma_{\mathrm{m}}\left\{1 - \left(\frac{y}{b}\right)^2\right\}\exp\left\{-\frac{1}{2}\left(\frac{y}{b}\right)^2\right\} \tag{10.2}$$

where σ_{m}, y, and b are peak tensile longitudinal RS, distance along y coordinate, and width of the tensile residual stress zone. Above expression for residual stress

is valid for fusion welded structures. But, given the similarity between the profiles of residual stresses in friction stir welding and fusion welding, the expression is expected to hold good for friction stir welded material also.

10.3 Measurement of Residual Stresses

Table 10.2 summarizes the techniques available to measure residual stresses and is classified into three groups: destructive, semi-destructive, and non-destructive. The intention here is to introduce some of the techniques used for residual stress measurement. Destructive methods involve the removal of material in a pre-conceived manner to assess uniaxial, biaxial, or triaxial stresses. In this method a priori knowledge of stress distribution is essential for selection of measurement technique to determine the stress state. Hole drilling and indentation are considered semi-destructive due to insignificant amount of material removal for residual stress measurements. X-ray diffraction, neutron diffraction, synchrotron diffraction, and ultrasonic wave velocity techniques are considered non-destructive since no material removal is required.

Although we are interested in residual stress distribution in essence all the techniques measures strain. The essential difference between destructive (or semi-destructive) and non-destructive methods is the manner in which the strains are measured for stress determination. To illustrate this point further, a schematic is drawn in Fig. 10.9. Here atoms and atomic bonds are represented by circles and springs. Figure 10.9a shows the material in relaxed state, i.e., in the absence of residual stress. Figure 10.9b represents a situation where residual stresses are present in the material. It is quite conceivable that the presence of stress in the material stretches the bonds, i.e., elastic strain exists. The non-destructive methods measure this strain. It is also possible to measure the strain by relaxing the stress. The stress relaxation is done by sectioning or material removal of the pre-stressed component. The material removal or sectioning results in relaxation of stretched bond, which is measured by strain gages. In relaxed state the state of the strain in a

Table 10.2 Residual stress measurement techniques

Method						
Destructive	Semi-destructive		Non-destructive			
Excision, sectioning, layer removal, tube splitting, crack compliance	Hole drilling, ring core	Indentation	X-ray diffraction	Neutron diffraction	Synchrotron diffraction	Ultrasonic wave velocity

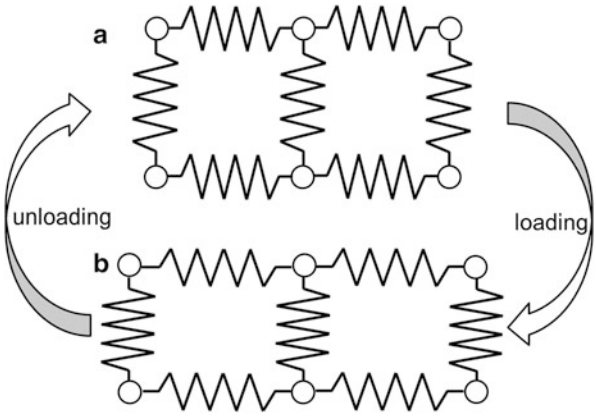

Fig. 10.9 Schematic to illustrate the change in state of strain in the material having residual stress. (**a**) relaxed state (**b**) loaded Circles and springs represent atoms and atomic bonds, respectively, between the atoms

material can be expressed by either Fig. 10.9a (when fully relaxed) or a state in-between Fig. 10.9a and b (when partially relaxed). Measurement of this change in elastic strain is the principle behind residual stress measurement using destructive or semi-destructive techniques.

Hole drilling and X-ray diffraction are by far the most widely used techniques for residual stress estimation and will be discussed below in some detail.

10.3.1 Hole Drilling

It is considered semi-destructive residual stress measurement technique and its widespread use stems from its simplicity and the use of inexpensive equipment in during the measurement. Two variants exist for this particular technique. In one procedure, a strain gage rosette is put around the region where stress measurement is to be done (Fig. 10.10a). A very small hole is drilled which results in relaxation of strain due to redistribution of stress in the region surrounding the hole. In another method, an annular groove is drilled around the strain gage rosette (Fig. 10.10a). It results in relaxation of strain in the material volume to which strain gages are attached. For a situation where there is no variation of stress along the depth of the specimen, the residual stresses at hole location can be measured using following expression for rectangular strain gage rosette (Schajer 2001),

$$\sigma_{\max}, \sigma_{\min} = -\frac{E}{2}\left(\frac{\varepsilon_3 + \varepsilon_1}{(1+\nu)\overline{a}} \mp \sqrt{\frac{(\varepsilon_3 - \varepsilon_1)^2 + (\varepsilon_3 + \varepsilon_1 - 2\varepsilon_2)^2}{\overline{b}}}\right) \tag{10.1}$$

Here, ε_1, ε_2, and ε_3 are elastic strain values measured using three strain gages in rectangular rosette. E and ν are elastic modulus and Poisson's ratio, respectively, of the specimen. $\overline{a}$ and $\overline{b}$ are calibration parameters which depend on the diameter and

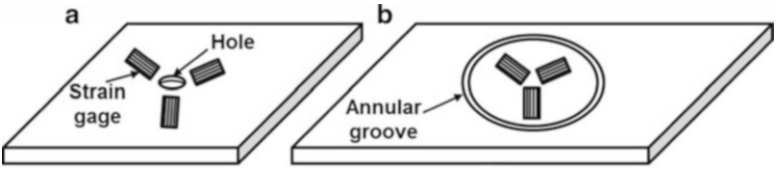

Fig. 10.10 A schematic showing strain gage rosette (**a**) around a hole drilled at the geometric center of the rosette and (**b**) within annular ring

depth of the drilled hole. For the situation where annular ring is drilled around the strain gage rosette and as a result complete relaxation of strain has taken place, the residual stresses is given by the expression (Schajer 2001),

$$\sigma_{\max}, \sigma_{\min} = -\frac{E}{2}\left(\frac{\varepsilon_3 + \varepsilon_1}{(1-\nu)} \mp \sqrt{\frac{(\varepsilon_3 - \varepsilon_1)^2 + (\varepsilon_3 + \varepsilon_1 - 2\varepsilon_2)^2}{(1+\nu)}}\right) \tag{10.2}$$

For the cases where significant stress gradient exists along the depth of the specimen other formulations of stress calculation based on strain measurements is used.

10.3.2 X-Ray Diffraction

As mentioned before, this is considered as a non-destructive technique, and is the most widely used method for residual stress measurement (Withers 2001). As explained using Fig. 10.9, in this case the strain is measured in the specimen in pre-stressed condition, which in turn is used to calculate stress. The strain is measured by measuring the interplanar spacings of different planes. For such purpose, X-rays are focused on the surface of the specimen on which residual stress measurement is to be done and intensity versus diffraction angle is recorded. Figure 10.11 shows the basic principle involved in the measurement of residual stresses using X-ray diffraction technique. It shows that once diffraction condition is met, X-ray gets diffracted from a set of crystallographic planes at an angle 2θ. This condition is given by the relationship proposed by Bragg,

$$\lambda = 2d_{hkl} \sin(\theta) \tag{10.3}$$

where λ, d_{hkl}, and θ are X-ray wavelength, interplanar spacing of plane {hkl}, and Bragg's angle, respectively. Equation (10.3) indicates that depending on the interplanar spacing the Bragg's angle would change. The interplanar spacing of a particular family of planes {hkl} depends on various factors such as composition, temperature, residual stress, etc. Hence, with regard to residual stress, the Bragg's angle for a set of planes {hkl} increases or decreases depending on whether the

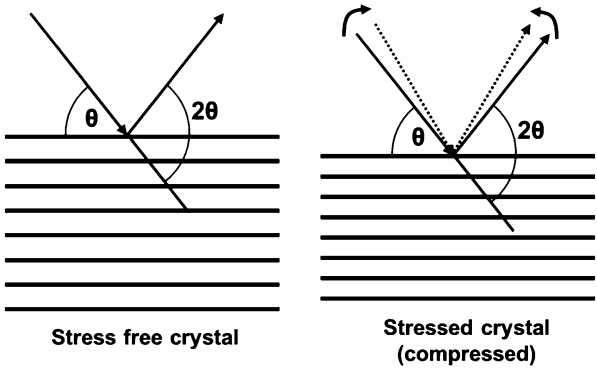

Fig. 10.11 Schematic illustration of basic principle X-ray diffraction in the measurement of residual stresses

existing stress has decreased or increased the interplanar spacing. Figure 10.11 shows how Bragg's angle increases for a sample under compressive loading. The strain perpendicular to the diffracting plane is calculated using following expression,

$$\varepsilon_i = \frac{d_{\mathrm{hkl}} - d_{0,\mathrm{hkl}}}{d_{0,\mathrm{hkl}}} \tag{10.4}$$

where $i = \mathrm{x}$, y coordinates. $d_{0,\mathrm{hkl}}$ is interplanar spacing of {hkl} family of planes in stress-free condition. The calculation of $d_{0,\mathrm{hkl}}$ should be performed in a region which is free from residual stress. As mentioned before, compositional changes and temperature might also affect the interplanar spacing. Hence, in a process like welding the interplanar spacing {hkl} across weld line is expected to be different even in the absence of residual stresses due to difference in microstructure in different regions. Therefore, interplanar spacing is measured in stress free condition in different microstructural states at multiple locations. Finally, the stresses are calculated using following relationship,

$$\sigma_{\mathrm{x}} = \frac{E}{(1-\nu^2)}\left(\varepsilon_{\mathrm{x}} + \nu\varepsilon_{\mathrm{y}}\right) \tag{10.5}$$

$$\sigma_{\mathrm{y}} = \frac{E}{(1-\nu^2)}\left(\varepsilon_{\mathrm{y}} + \nu\varepsilon_{\mathrm{x}}\right) \tag{10.6}$$

where ν is Poisson's ratio. Since, X-ray diffraction measures the stress at the surface of a component where essentially biaxial stress of state exists, Eqs. (10.5) and (10.6) are adequate to compute both components of the residual stress. There are situations where stresses within the penetration depth of X-rays (~100 μm), may exist perpendicular to the plane of residual stress measurement. In such cases, biaxial assumptions might not hold good. In such cases, triaxial method should be invoked to calculate all three components of stresses.

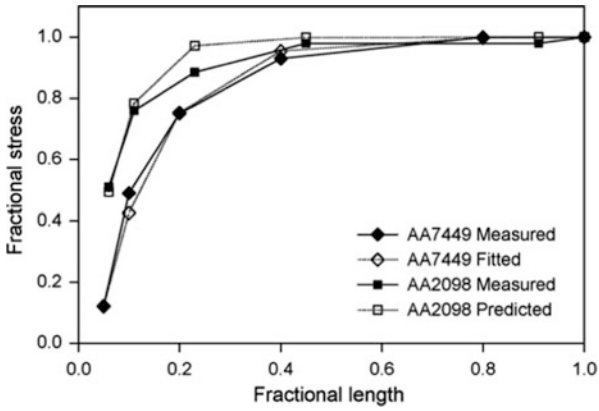

Fig. 10.12 Effect of sectioning on the longitudinal residual stress distribution in the weldments (Altenkirch et al. 2008, 2009b, reprinted with permission from Elsevier)

10.3.3 Role of Sample Size in the Measurement of Residual Stresses

The literature shows that different sample sizes have been used for measurement of residual stresses. In this section we will see how the sample size used for the measurement purposes can affect the outcome of the measurement. Different size samples are chosen either due to the constraint imposed by the measurement devices or a correlation needs to be established between residual stress and a particular property of the material. It is well-documented in literature that sectioning of the welded samples lead to relaxation of residual stresses. To illustrate this point further, the work done by Altenkirch et al. (Altenkirch et al. 2008, 2009b) on AA7449 and AA2098 alloys are included in Fig. 10.12. It shows the stress remaining (fractional stress defined as the ratio of stress remaining and stress at the weld centerline in as-welded condition) at weld centerline as a function of fractional length of the plate. It is evident that the original stress level is maintained up to 40 % fractional length of the plate. When fraction length reaches below 10 % of the original length, the remnant residual stresses at weld centerline were ~50 % and ~10 % for AA2098 and AA7449 alloys, respectively.

The experimentally measured curve can be curve fitted with following empirical expression,

$$\sigma_{relax} = \sigma_o \left[1 - \exp\left(-\frac{l_r - l_{relax}}{l_{char}}\right)\right] \tag{10.7}$$

where σ_{relax}, σ_0, l_r, l_{relax}, and l_{char} are stress at the weld centerline after sectioning, stress at the weld centerline in as-welded condition, remaining length, length at which RS becomes zero, and characteristics distance beyond which sectioning does not influence RS distribution, respectively.

This example exemplifies the role sample dimensions play in the measurement of residual stresses. Therefore, a careful selection of sample size to obtain representative residual stress measurement is required.

10.4 Effect of Residual Stress on Properties

Figure 10.13 shows pictorially the properties which may get influenced by the presence of residual stresses. However, the evaluation of the influence of the residual stress on these properties is very difficult because these properties (except dimensional stability) are not only dependent on the level of such stresses but also on the microstructural state of the alloy. Any welding technique including friction stir welding modifies the microstructure in the welded zone. Hence, a great care should be exercised while interpreting the results on the influence of residual stresses on the properties mentioned in Fig. 10.13.

Figure 10.14 shows how presence of residual stresses can alter the buckling strength of a material. Figure 10.14a shows a slender cylindrical bar under compressive load. The bar contains a compressive residual stress oriented along the loading direction. The material shows elastic-perfectly plastic deformation behavior. Figure 10.14b shows two different stress-strain curves. In the absence of any residual stress, the bar being made of elastic-perfectly plastic material, follows the path OA'AB'B. However, in the presence of a compressive residual stress of magnitude

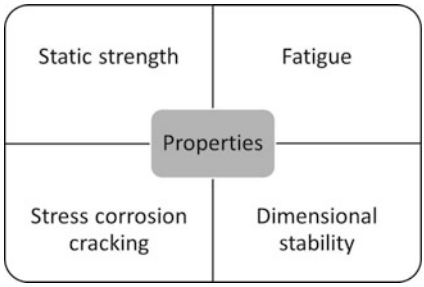

Fig. 10.13 Some properties which may get affected by the presence of residual stresses

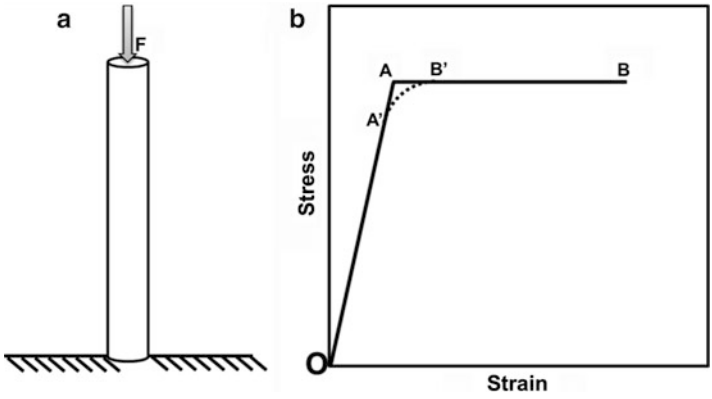

Fig. 10.14 (**a**) A cylindrical bar containing compressive residual stress along the axis of the cylinder experiencing compressive loading. (**b**) Modification of stress-strain curve due to the presence of residual stresses (Adapted from Masubuchi 1980b)

σ_{rs} the material takes the path OA'B'B during deformation. Point A in the stress-strain curve represents yield strength (σ_Y) of the material. However, in the presence of residual stress, the yield strength of the material is below point A, i.e., when $\sigma + \sigma_{rs}$ equals to σ_Y. It implies that applied stress σ is lower than σ_Y. This point corresponds to A' in the stress-strain curve in Fig. 10.14b. Another interesting feature which can be noted is decreasing influence of residual stress with continued plastic deformation. At point B' the influence of residual stress on flow stress vanishes completely.

Similarly, fatigue properties are strongly affected by the presence of residual stresses. However, quantification of such change is not an easy task. Welding process not only introduces residual stresses in a component but also modifies microstructure in the welded zone. Residual stress and change in microstructure both modify the fatigue deformation behavior of welded materials. Researchers have tried deconvoluting these two components and studied impact of each on fatigue crack growth rate (Bussu and Irving 2003; Pouget and Reynolds 2008; Fratini et al. 2009). To study the effect of microstructure on fatigue crack growth rate, it can be subjected to heat treatment to relieve the stresses. However, it should be ensured that the microstructure does not change to the extent that it changes the properties of the material significantly from the one obtained in as-welded condition. Another means by which residual stresses can be relieved is by deforming the welded workpiece plastically. This also should be done in such a way that microstructure and hence mechanical properties are still representative of as-welded condition. The difference in the crack growth rates in as-welded and stress-relieved conditions can be used to elucidate the role of residual stresses on the fatigue deformation behavior. In friction stir welded plates, it has been found that crack growth rate is slower in heat-affected zone and faster in nugget compared to base material. Data contradicting the trend observed for crack growth rate in different zone have also been reported in literature.

10.5 Dependence of Residual Stresses on Friction Stir Welding Parameters

As mentioned before there are number of processing parameters which affect the state of residual stresses and resulting distortion of a friction stir welded plate. Figure 10.15 summarizes all the parameters which may affect generation of residual stresses in friction stir weldments. It is evident that all these parameters can affect the thermal profile during friction stir welding process. As we know thermal excursion has profound impact on the generation of residual stresses and any modification in it would have bearing on the thermal stresses and hence residual stresses. Although all the parameters mentioned in Fig. 10.15 may affect the residual stresses, the role of tool traverse speed and tool rotation rate are most widely studied in this context.

Figure 10.16 illustrates the effect of tool rotation rate on residual stresses. In this particular example a 5083Al-H321 plate was used for welding. Feed rate (tool

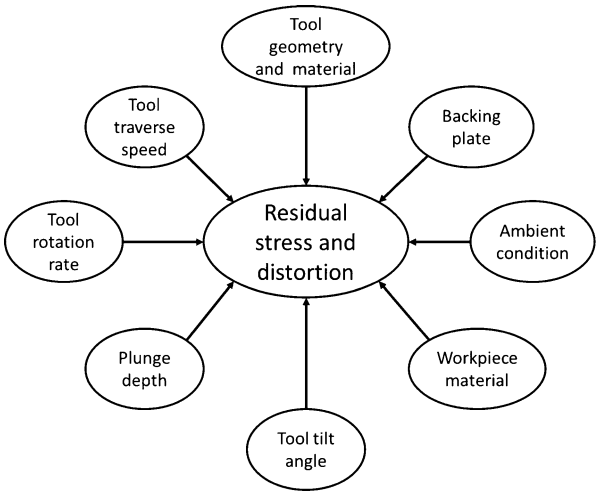

Fig. 10.15 Schematic illustration of the parameters affecting residual stresses and distortions in the welded component

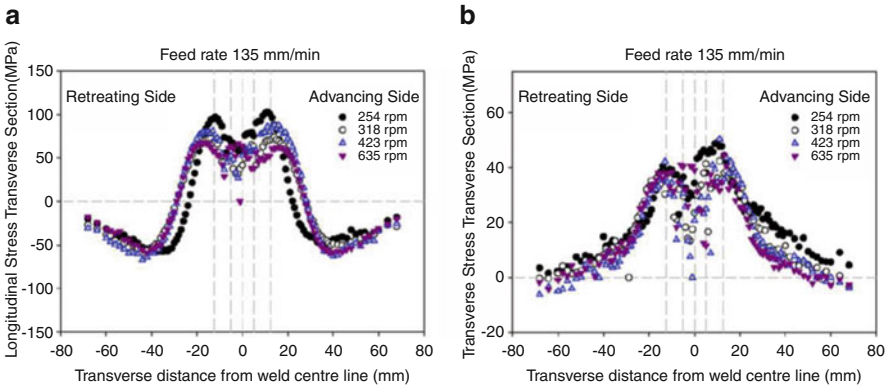

Fig. 10.16 Effect of tool rotation rate on (**a**) longitudinal and (**b**) transverse residual stresses in 5083Al alloy (Lombard et al. 2009, reprinted with permission from Elsevier)

traverse speed) and tool rotation rates were variables (Lombard et al. 2009). Figure 10.16 shows the variation in longitudinal and transverse residual stress for tool rotation rates ranging from 254 to 635 rpm at a constant feed rate of 135 mm/min. It shows a systematic decrease in peak and weld centerline longitudinal residual stress values (Fig. 10.16a) with increase in tool rotation rate. Other point which can be noted is increase in the width of welded region containing longitudinal tensile residual stresses. However, the increase of the width is not monotonic. For tool rotation rate 318 rpm and above, no increase in the width of the zone containing longitudinal tensile residual stresses. The variation of transverse residual stress across the weld centerline as a function of tool rotation rate is not

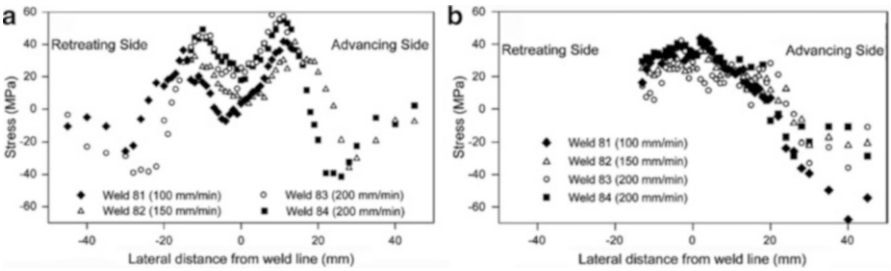

Fig. 10.17 Effect of tool traverse speed on the distribution of (**a**) longitudinal and (**b**) transverse residual stresses across the width of 5083Al weld (Peel et al. 2003, reprinted with permission from Elsevier)

well defined. However, as reported in literature, here also overall the longitudinal residual stresses are greater than the transverse residual stresses.

The observed trend as a function of tool rotation rate can be rationalized as follows. In general, increasing tool rotation rate causes the peak temperature in the plate being welded to rise. The degree of annealing and consequently thermal stress relieving is more at higher peak temperature for the material volume on the trailing side in the wake of the friction stir welding tool. This results in a decrease in residual stress. Higher peak temperature may also cause higher width of the nugget which will, in turn, increase the width of the zone containing tensile longitudinal residual stresses.

Similar to the tool rotation rate, the variation in the feed rate or the tool traverse speed also brings about changes in the distribution of residual stresses in the welded specimens. Figure 10.17 shows changes in the distribution of residual stresses as a function of tool traverse speed (Peel et al. 2003). Overall, a decrease in longitudinal residual stresses can be noted from Fig. 10.17a with decrease in tool rotation rate. As was the case with the change in tool rotation rate, in this case also no general trend could be observed in the case of transverse residual stresses with change in tool traverse speed.

A decreasing tool traverse speed causes higher heat input in the material during welding. It causes temperature to go up in the sample being welded. As mentioned before, a higher peak temperature would have higher thermal stress relieving effect on the material volume on the trailing side of the friction stir welding tool. Hence, thermal stress relieving effect would cause a lower residual stresses at lower tool rotation rate.

Figure 10.17 also includes effect of tool geometry on residual stresses. The weld number 83 and 84 were made at 200 mm/min tool traverse speed. However, the diameter and pitch of the thread of the tool pin were 5.0 mm and 0.8 mm, respectively for weld 83. For weld 84, the tool pin was 6 mm in diameter and had 1.0 mm pitch of the thread. The careful observation of the results presented for these cases suggest not much dependence of residual stress distribution on pin geometries. Given that the contribution of the tool pin to the total heat input is very small compared to the contribution made by the shoulder of the tool, such a small

variation in the geometry may not cause much change in the distribution and values of the residual stresses.

Section 10.3.3 discussed the effect of sample dimensions on the measurement of residual stresses. The sectioning of the welded samples for residual stress measurement results in stress relaxation due to reduced stiffness of the welded materials. Similarly, if a relatively smaller component is welded, it will impose less constraint on the contracting welded zone (to be discussed in Sect. 10.6). It, therefore, results in the development of residual stresses of smaller magnitude. As sample dimensions are increased, the material surrounding welded zone will impose increasingly higher level of constraints, thereby making contraction of the welded zone more difficult. Hence, it would result in the development of higher level of residual stresses. Although larger samples may introduce very high level of residual stresses, they present higher resistance to distortion due to higher cross-section or geometry related stiffness.

There is complete lack of a systematic study involving role of welding coupon size on the development of residual stresses. It is also worth mentioning that the experimental approach to address this issue would be a painstaking task. Given the current state-of-the-art of numerical methods, it would be a viable option to explore the role of coupon size numerically on the residual stresses and resulting distortions (Section 10.9).

10.6 Understanding Development of Residual Stresses in Friction Stir Welding

An understanding about the origin of residual stresses in welded components is of paramount importance and is key to mitigating residual stresses in the weldments and hence distortions. For this purpose a conceptual model is presented in Fig. 10.18. A rectangular bar of length l_o and width w is shown to be sandwiched between two rigid constraints (no deformation of the constraints) at the opposite end of the bar. When the temperature of an unconstrained bar is raised by T (Fig. 10.18b), it will elongate and the change in length is given by

$$\Delta l = l_o(1 + \alpha \Delta \mathrm{T}) \tag{10.8}$$

where Δl, l_o, α, and ΔT are change in length, initial length, coefficient of thermal expansion, and difference between final and initial temperature of the bar, respectively. In the absence of any constraints, the bar is free to expand. However, when constraints are present, $\Delta l = 0$. Due to which the bar would be subjected to compressive stress and strain. If temperature is raised sufficiently the bar might undergo plastic deformation.

Figure 10.18c, d describe a situation where such constraints have been removed at the end and $\Delta \mathrm{T} = 0$. If during heating ΔT was such that it deformed the bar only elastically, it will regain original dimension once $\Delta \mathrm{T} = 0$ (Fig. 10.18c). However, if

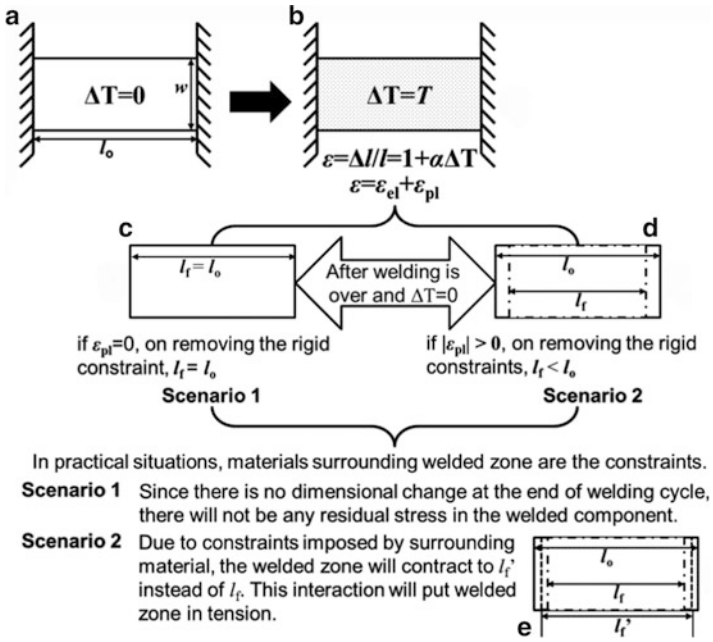

Fig. 10.18 A conceptual model to understand the development of residual stresses in friction stir welding, (**a**) A workpiece at room temperature, (**b**) workpiece heated to a temperature T, (**c**) workpiece showing original length regained after the welding, if $\varepsilon_{pl} = 0$, (**d**) workpiece comparing the length before and after welding if $|\varepsilon_{pl}| > 0$, (e) effect of constraints on the dimensional change

the change in ΔT (Fig. 10.18b) leads to plastic deformation of the bar, it would like to contract on removal of the constraint as it cools down so that eventually $\Delta T = 0$ (Fig. 10.18d). It contracts because the presence of rigid constraints places the bar in compressive state of stress and it results in compressive plastic strains in the bar. Hence, on removal of such constraints during cooling of the bar, it tries to contract. In both the cases since bar is allowed to achieve it equilibrium shape, it will be free from any residual stresses. In actual situations, for example, during welding, it is not possible to get rid of constrains completely. The material surrounding the welded zone will always impose some level of constraint on welded zone and would lead to introduction of residual stresses. The level of residual stresses will now depend of the extent of constraints imposed on the welded zone.

Scenario 1 in Fig. 10.18 describes a situation where bar was subjected to elastic compressive strain due to heating of the bar. If this strain is relaxed completely, there should not be any residual stress when all the external forces have been removed. In scenario 2 which refers to the case presented in Fig. 10.18d, it is shown in Fig. 10.18e that if the contraction of the bar takes place in constrained condition (constraints not shown), it will lead to tensile stresses in the welded zone.

This conceptual model suggests that compressive plastic strains accumulated during the thermal cycle, where flow stress of the material is lower than the thermal

stresses, in the welded zone are responsible for tensile residual stresses developed in the welded zone. Hence, mitigation strategies should be directed towards reduction or removal of such tensile stresses due to dimensional mismatch between welded zone and surrounding materials. In Sect. 10.8 where mitigation efforts have been presented, it will be discussed how those techniques help reduce such dimensional mismatch in different regions of the weld and hence influence the residual stress and distortion of the weldments.

10.7 Difference Between Residual Stress Generation in Friction Stir Welding and Fusion Welding

There are a few subtle differences in the manner in which residual stresses develop during fusion welding and friction stir welding. Figure 10.19 illustrates the deformation of the plate being welded using friction stir and fusion welding techniques. Figure 10.19a, b show that compressive plastic deformation (equivalent plastic strain) of the plate during welding starts when thermal stresses (Mises stress) become equal (point B) to the yield stress of the material. It is shown that thermal stresses increase and yield stress of the material decreases as temperature rises in the material. As long as thermal stresses are equal to the yield strength of the material, plastic strain keeps on accumulating in the welded region. During cooling cycle yield strength of the material starts to rise and a point is reached where it is higher than thermal stresses in the material. From this point onward the plastic deformation of the plate stops at the location under consideration.

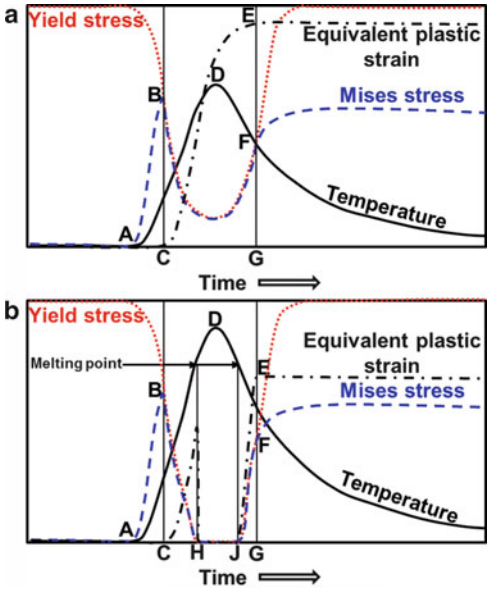

Fig. 10.19 Schematic illustrating the possible difference in residual stress generation between friction stir welding (solid state) and fusion welding; (**a**) Friction stir welding and (**b**) fusion welding

Friction stir welding being a solid-state joining technique peak temperature in the processed zone never exceeds melting point of the material. As name implies, in fusion welding temperature reaches well above melting point of the material. Comparison of Fig. 10.19a, b indicate that the compressive plastic strain continues to accumulate until thermal stresses become smaller than yield strength of the material in FSW (point F). For fusion welding it drops to zero when temperature exceeds the melting point of the material. In this case plastic strain again starts accumulating once solidification of melt pool starts and continues as along as yield strength and thermal stresses are equal (up to point F in Fig. 10.19b).

The compressive plastic deformation leads to a geometrical misfit between welded region and the material surrounding it. It eventually results in generation of tensile stresses in the welded region and compressive stresses in the regions away. Another source which adds to geometrical misfit emanates from solidification shrinkage of the melt pool. Shrinkage takes place due to material loss as a result of evaporation, spattering, etc. Hence, in friction stir welding the misfit occurs mostly due to compressive plastic deformation of the welded region, whereas it occurs due to combined effect of compressive plastic strain and solidification shrinkage in fusion welded structures.

10.8 Mitigation of Residual Stresses

A number of techniques such as thermal tensioning, active cooling, weld sequencing, precambering, post-weld heat treatment, etc. have been employed to mitigate residual stresses and resulting distortions of the welded structures using fusion welding. Some of these techniques have been utilized in friction stir welding also for the management of residual stresses and distortions. Some of these techniques will be described here.

10.8.1 Active Cooling

It is an in-situ technique used for mitigating residual stresses and hence distortion. As the name suggests, the mitigation is effected by modifying the existing thermal field due to friction stir welding by imposing an external source of cooling (active cooling).

The active cooling technique is described schematically in Fig. 10.20. Liquid nitrogen, liquid CO_2, and water are few examples of cooling media. Although, Fig. 10.20 shows location of the cooling nozzle on the trailing side of FSW tool, it can be anywhere in the vicinity of the tool. But, limited research has shown that location of the tool with respect to FSW tool is very important. In Sect. 10.9 the results of finite element analysis on the effect of location and number of nozzles are discussed. The use of cooling media basically modifies the thermal field (favorably) around the tool thereby reducing geometrical misfit between the welded zone and

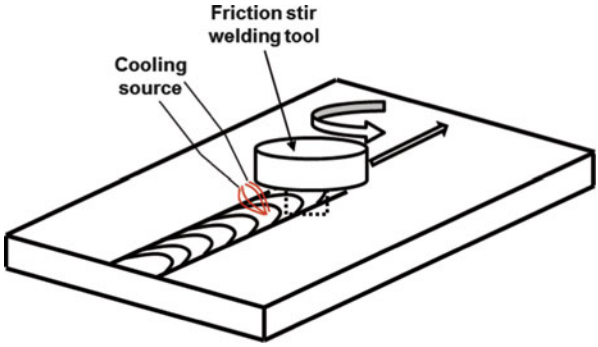

Fig. 10.20 Schematic illustration of deployment of active cooling source to mitigate residual stress

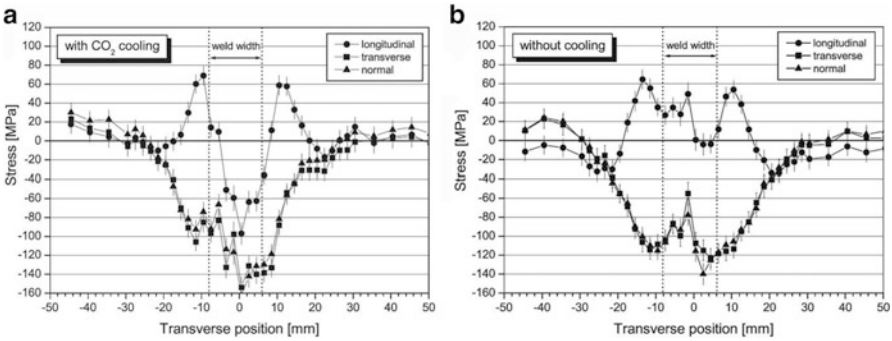

Fig. 10.21 Residual stress mitigation by the use of active cooling (in-situ cooling using liquid CO_2) on the trailing side of the tool; material: 2024Al-T351; residual stress distribution (**a**) with cooling and (**b**) without cooling (Staron et al. 2002, reprinted with permission from Springer)

the surrounding material. The reduction results in lower level of residual stresses in the welded structure.

Figure 10.21 provides an example of the effect of deployment of such active cooling media on the residual stress distribution (Staron et al. 2002). Figure 10.21a corresponds to the case where liquid CO_2 was used to mitigate residual stress. In the welded region all three (x, y, and z) components of the residual stress are compressive. However, for the case where welding was done without the aid of active cooling medium (Fig. 10.21b) the longitudinal residual stresses are tensile in nature. Evidently, the use of cooling medium during friction stir welding is an effective means of managing the distribution of residual stresses in welded structures.

10.8.2 Mechanical Tensioning

This is also a very effective technique for managing the distribution of residual stresses in welded components. A schematic of this technique is illustrated in Fig. 10.22. In this technique the plates being welded are subjected to tensile loading. The magnitude of

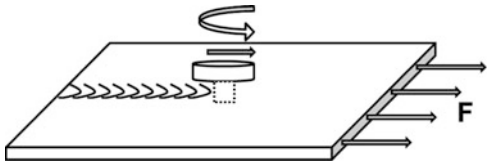

Fig. 10.22 Schematic illustration of mechanical tensioning technique

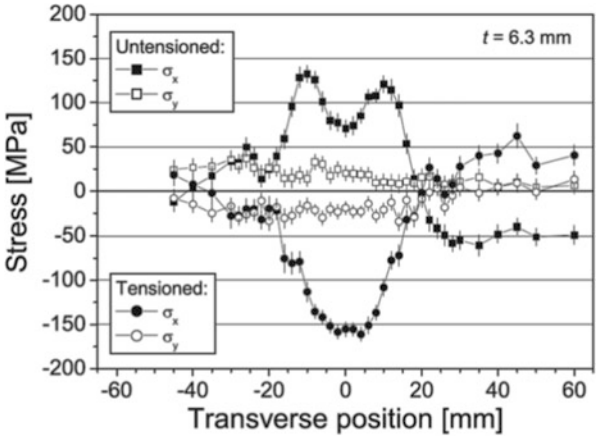

Fig. 10.23 Residual stress management in 2024Al-T351 alloy by the use of roller tensioning technique (Staron et al. 2004, reprinted with permission from Elsevier)

loading can be from a small fraction to a significant proportion of the yield strength of the material. Due to in-situ loading compressive plastic deformation ahead of FSW tool decreases whereas tensile plastic deformation or yielding behind the tool increases. It results in lower misfit between welded zone and surrounding materials. This technique can be applied after welding also. However, the load requirement increases due to higher strength of the welded zone at low temperature.

Figure 10.23 illustrates the effect of mechanical tensioning on the components of residual stress in 2024Al plate (Staron et al. 2004). Clearly, both longitudinal and transverse residual stresses are tensile in nature in major parts of the plate. However, after subjecting it to a tensile load 70 % of yield strength of 2024Al-T351 at room temperature, the nature of residual stresses change from tensile to compressive for both the components of the residual stress.

10.8.3 Roller Tensioning

The mechanical tensioning method described above is also known as global mechanical tensioning method because entire weld plate is loaded simultaneously. As opposed to this, roller tensioning technique is regarded as local mechanical tensioning method as it stretches weld material at the location the rollers are present.

Figure 10.24 describes roller tensioning technique. Use of single roller right in the welded zone is shown in Fig. 10.24a. This particular situation can be implemented either in-situ or post welding. Instead of directly moving the roller

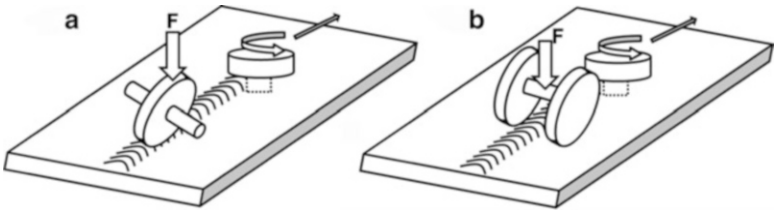

Fig. 10.24 Schematic illustration of roller tensioning technique; (**a**) rolling of the weld beam—in-situ and post-weld both possible and (**b**) rolling of the material adjoining welded zone (adapted from Altenkirch et al. 2009a)

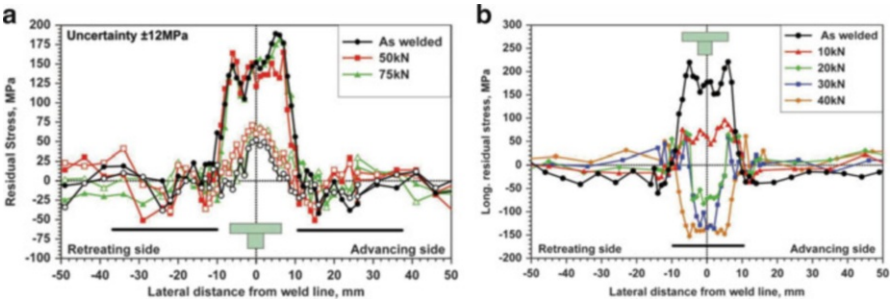

Fig. 10.25 (**a**) In-situ roller tensioning (Fig. 10.24b) and (**b**) post-weld roller tensioning (Fig. 10.24a) (Altenkirch et al. 2009a, reprinted with permission from Maney Publishing)

over the welded zone, it can also be made to move in the zone next to it. This particular scenario is shown in Fig. 10.24b where two rollers are moving just next to the welded region.

Figure 10.25 shows experimental results following roller tensioning technique to mitigate residual stress (Altenkirch et al. 2009a). It shows that in-situ roller tensioning (Fig. 10.24b) did not cause any change in the distribution of residual stresses across the width of the plate. However, when roller tensioning was applied post-weld, it resulted in not only reduction in the magnitude of residual stresses in welded zone but also changed the nature of the residual stress at sufficiently higher loads.

10.9 Modeling and Simulation of Residual Stresses in Friction Stir Welding

With the advent of modern computers, modeling and simulation has become an integral tool in many engineering applications. In parallel there has been a great deal of development activities in the area of commercial numerical codes which are assisting in many engineering design and development works in various disciplines. The application of modeling and simulation technique in the study of residual stress

and resulting distortion is no exception. Although, in last two decades or so, there has been a surge in modeling activities relating to weld residual stress and distortion, it has been actively pursued for last four decades (Michaleris 2011).

The residual stress and distortion study of fusion welding processes carried out through modeling and simulation has greatly benefitted similar studies in friction stir welding. In fusion welding techniques mostly Eulerian frame of reference where material and mesh are not associated is used for this purpose using computational fluid dynamics (CFD) technique. Although, CFD is capable of providing us with thermal history and profile of the weld pool during fusion welding, it does not provide any information on residual stresses. However, the thermal history obtained in CFD can be used as an input to another finite element code utilizing elastoplastic material model in Lagrangian frame of reference. Friction stir welding being a solid-state joining technique directly utilizes conventional elastoplastic analysis technique in the prediction of residual stresses and distortions. It is worth mentioning that similar to that in fusion welding technique, use of CFD followed by elastoplastic model has been incorporated in friction stir welding also to study residual stresses (Richards et al. 2010).

Despite significant improvement in computational speed, the computational cost is still very high due to complexity of the processes like friction stir welding. Hence, during the modeling of the process a great number of assumptions are made to keep the size of the problem as minimum as possible. But, at the same time efforts are directed towards keeping all the essential components of a process intact so that the output of the modeling still remains meaningful. Chao and Qi (1998) were first to study the residual stress and distortions in 6061Al. In the plate only conduction mode of heat transfer was considered. The heat transfer to ambient air from top surface and to the backing plate from bottom of the plate were modeled using appropriate heat transfer coefficients. The heat transfer to the tool was not considered. A moving heat source was considered to model the actual friction stir tool. Such a heat source is capable of mimicking the heat generated by frictional and adiabatic plastic deformation of the material surrounding the tool. However, the actual plastic deformation cannot be modeled. In this particular case total heat input was varied until computational and thermal temperature profiles matched well. It was a sequentially coupled thermo-mechanical analysis. Thermal analysis was followed by stress analysis in the plate. Recent finite element models are able to introduce more sophistication in the analysis with reduced time for the analysis (Buffa et al. 2006, 2011). For example, it is now possible to include plunge stage, tool extraction stage, and plastic deformation by the tool during different stages of friction stir welding process. However, it should be mentioned that for residual stress modeling it is not important to include plastic deformation due to the tool movement. The incorporation of plastic deformation may become important in cases where knowledge of strain, strain rate, and adiabatic heat generated due to plastic deformation may be necessary. Although, it is possible to consider volumetric heat generation to include the heat generation at tool pin/workpiece interface, this part also can be ignored for residual stress modeling purpose leading to further simplification of the analysis. Buffa et al. (2008) showed by processing 7075Al-T6 with pin and pinless tool that

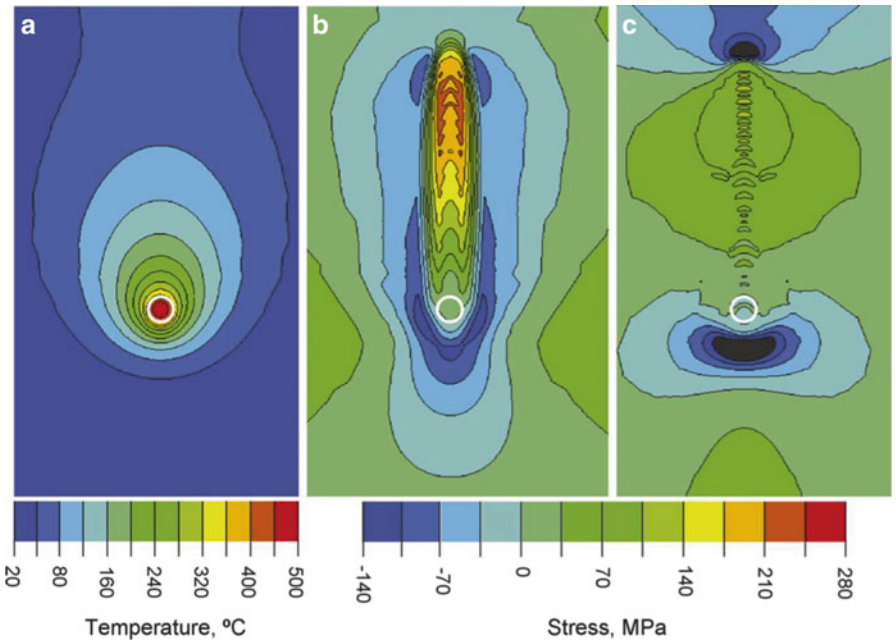

Fig. 10.26 Contour plots of temperature and thermal stresses in 2024Al-T6 plate. A heat input of 958 W was used in the simulation. (**a**) Temperature contour plot, (**b**) longitudinal stress distribution, and (**c**) transverse stress distribution (Richards et al. 2008, reprinted with permission from Elsevier)

the longitudinal residual stress distribution was same in both the cases. The main conclusion of this work was that the residual stress is mainly affected by heat generated at tool shoulder/workpiece interface. In fact, a very good correlation between modeling based on surface heat source and experimental residual stress measurement results is another validity of such assumptions.

Figure 10.26 shows the two-dimensional contour plot of temperature and thermal stress in a 2024Al-T6 plate (Richards et al. 2008). The temperature profile and residual stress distribution corresponds to 770 rpm and 195 mm/min friction stir welding parameters. It corresponds to a weld power of 958 W. The power was obtained using a heat transfer model using CFD technique. The thermal profile obtained from the CFD based heat transfer model was used as an input in a three dimensional stress analysis model designed to compute residual stresses. It should be noted that away from the tool (shown by white circular region in the figure) stresses are tensile and ahead of the tool thermal stresses are compressive in nature. Experimentally it is possible to get the knowledge on the thermal stress evolution only at selected locations. However, this example shows that computationally we get far greater insight into the evolution of thermal and, as will be shown next, residual stresses.

Figure 10.27 shows distribution of computed residual stress (longitudinal and transverse) in SS 304L. The processing condition of the stainless steel sheet is

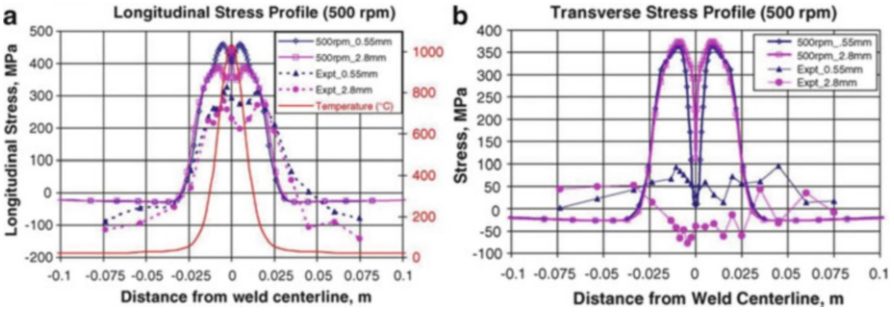

Fig. 10.27 Residual stress distribution in a stainless steel 304L; (**a**) Longitudinal and (**b**) transverse stresses. Experimental condition: Plate thickness 3.2 mm, tool rotation rate 500 rpm, tool traverse speed 4 ipm (102 mm/min), length of the welded region 279 mm (Khandkar et al. 2006, reprinted with permission from Elsevier)

provided in the caption of Fig. 10.27. The residual stress values are reported for different depths: 0.55 and 2.8 mm below top surface of the sheet. The experimental residual stress data are also superimposed to compare them with computed stress distribution profile. As can be noted here the longitudinal residual stress prediction is quite well. However, the predicted transverse residual stress varies significantly in the close vicinity of the weld centerline. Boundary conditions used at weld centerline (or plane of symmetry), neglecting tool movement assisted plastic deformation, and lack of some temperature dependent physical and mechanical properties for the alloy are a few possible reasons for the deviation of predicted transverse residual stresses from the experimentally measured one.

Previous couple of examples demonstrated how modeling and simulation work is assisting us in visualizing thermal and residual stress generation during friction stir welding. In next couple of examples it will be demonstrated how residual stress simulation work is assisting in taking steps to mitigate residual stresses and resulting distortion. Section 10.8 discussed various experimental approaches undertaken to mitigate residual stresses in welded components. Here finite element study of global mechanical tensioning and the role of active cooling in addressing the issue of residual stress and resulting distortions of welded components will be illustrated. Active cooling (use of cooling media such as liquid CO_2, liquid nitrogen, etc.) has been used for reducing or eliminating residual stresses in friction stir welded components by many. Richards et al. (2010) studied this aspect using finite element method in a 2024Al-T3 plate. The effect of the location of a cooling nozzle on the thermal contour profiles are shown in Fig. 10.28. Figure 10.28a is a contour plot without any active cooling. Figure 10.28b represents a situation where the cooling nozzle was placed in front of the heat source which is equivalent of placing it ahead of friction stir welding tool. The effect of the presence of cooling nozzle on thermal profiles is quite evident from these images. The effect of active cooling and its position with respect to the heat source is illustrated in Fig. 10.29. It is quite remarkable to note the inversion of the nature of longitudinal residual stress at the weld centerline. It changes from a tensile value close to 130–135 MPa to compressive 20 MPa.

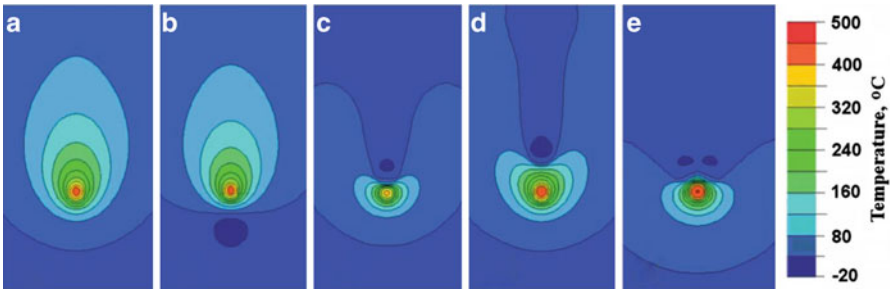

Fig. 10.28 Temperature contour plot as a function of distance of cooling nozzle from heat source; (**a**) no cooling, (**b**) 20 mm in front of the heat source; in rest of the cases heat cooling source behind the heat source (**c**) 20 mm, (**d**) 40 mm, and (**e**) two heat sinks at 20 mm (Richards et al. 2010, reprinted with permission from Maney Publishing)

Fig. 10.29 Effect of active cooling and the position of the cooling medium on the longitudinal residual stress distribution. The distribution is at mid-thickness level halfway along the length of the plate (Richards et al. 2010, reprinted with permission from Maney Publishing)

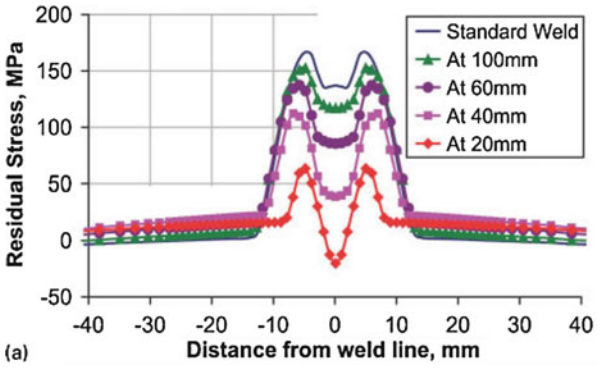

As mentioned before global mechanical tensioning is another method of reducing residual stresses in the welded components, and this has been studied using finite element methods. As an example the result of the study done by Richards et al. (2008) is included here in Fig. 10.30. It shows two dimensional longitudinal stress and plastic strain distributions as a function of applied in-situ tensile load. After tensioning to 35 % of the yield strength of 2024Al-T6 at room temperature, Fig. 10.30b shows close to zero plastic strain. At this level of tensioning the longitudinal stresses are also very small. The tensioning level with respect to room temperature yield strength might change depending on the exact processing condition. Experimentally also it has been observed that at tensioning level ranging from 25 to 50 % of room temperature yield strength, the residual stresses were close to zero (Staron et al. 2004; Altenkirch et al. 2008; Price 2007).

Hence, it is quite evident from above examples that finite element simulation study of residual stresses in friction stir welding is assisting not only in developing an understanding of process parameter affecting the residual stresses but also suggesting means of mitigating such stresses.